

# RNA-binding specificity of *E. coli* NusA

Stefan Prasch<sup>1,\*</sup>, Marcel Jurk<sup>1</sup>, Robert S. Washburn<sup>2</sup>, Max E. Gottesman<sup>2</sup>,  
Birgitta M. Wöhrl<sup>1</sup> and Paul Rösch<sup>1</sup>

<sup>1</sup>Lehrstuhl für Struktur und Chemie der Biopolymere & Research Center for Bio-Macromolecules, Universität Bayreuth, Universitätsstrasse 30, 95447 Bayreuth, Germany and <sup>2</sup>Department of Microbiology and Institute of Cancer Research, Columbia University Medical Center, New York, NY 10032, USA

Received March 18, 2009; Revised May 12, 2009; Accepted May 13, 2009

## ABSTRACT

The RNA sequences *boxA*, *boxB* and *boxC* constitute the *nut* regions of phage  $\lambda$ . They nucleate the formation of a termination-resistant RNA polymerase complex on the  $\lambda$  chromosome. The complex includes *E. coli* proteins NusA, NusB, NusG and NusE, and the  $\lambda$  N protein. A complex that includes the Nus proteins and other factors forms at the *rrn* leader. Whereas RNA-binding by NusB and NusE has been described in quantitative terms, the interaction of NusA with these RNA sequences is less defined. Isotropic as well as anisotropic fluorescence equilibrium titrations show that NusA binds only the *nut* spacer sequence between *boxA* and *boxB*. Thus, *nutR boxA5-spacer*, *nutR boxA16-spacer* and *nutR boxA69-spacer* retain NusA binding, whereas a *spacer* mutation eliminates complex formation. The affinity of NusA for *nutL* is 50% higher than for *nutR*. In contrast, *rrn boxA*, which includes an additional U residue, binds NusA in the absence of *spacer*. The  $K_d$  values obtained for *rrn boxA* and *rrn boxA-spacer* are 19-fold and 8-fold lower, respectively, than those for *nutR boxA-spacer*. These differences may explain why  $\lambda$  requires an additional protein,  $\lambda$  N, to suppress termination. Knowledge of the different affinities now describes the assembly of the anti-termination complex in quantitative terms.

## INTRODUCTION

Gene expression in *Escherichia coli* and its phage can be controlled at the level of transcription termination. The best-studied examples of this mechanism are the ribosomal operons (*rrn*) and the bacteriophage  $\lambda$  (1–3). Transcription of the *E. coli rrn* operons is in part regulated by suppression of termination (anti-termination) (4). Anti-termination in *rrn* is mediated by an RNA recognition sequence (AT) located just distal to the promoters, close

to the 5' end of the pre-rRNA transcript (Figure 1A). A number of factors, including NusA, NusB, NusE (ribosomal protein S10) and NusG, modify RNA polymerase (RNAP) at AT. The modified RNAP is insensitive to termination by Rho-dependent terminators that occur throughout the long pre-rRNA transcript. AT includes a highly conserved sequence (*boxA*) that binds NusB, NusE and NusB–NusE complex (5,6). Distal to AT is an additional conserved sequence (*boxC*) that is less well characterized, but is a specific binding site for NusA in *Mycobacterium tuberculosis rrn* (7). Two short oligo ribonucleotides derived from the *boxC* stem-loop motif bind exclusively to the two KH domains of NusA in a completely extended conformation, and adenine-backbone interactions with the trinucleotide sequence AUA are particularly critical for this interaction (8).

Gene expression in lambdoid phages is also controlled by anti-termination. The Nus proteins form a complex with and modify RNAP at the  $\lambda$  *nutL* and *nutR* sequences. *nutL* and *nutR* consist of *boxA*, a *spacer*, a stem-loop element (*boxB*), and *boxC* (Figure 1B). The *rrn boxA* (5'-UGCUCUUUA-3') and the  $\lambda$  *boxA* (5'-CGCUCUUUA-3') differ; the CUUUA of *rrn boxA* is thought to enhance anti-termination efficiency (9).  $\lambda$  and other lambdoid phages express N, an RNA-binding protein of the arginine-rich motif (ARM) family, that binds *boxB* (10–13). N is required for anti-termination on the  $\lambda$  chromosome. (14). In both the *rrn* and  $\lambda$  anti-termination systems, the modified RNAP retains the ability to transcribe through multiple terminators. However, *rrn* anti-termination is effective only at Rho-dependent terminators, whereas  $\lambda$  anti-termination complexes are highly resistant to both Rho-dependent and Rho-independent terminators (15).

The *nut* sequences and the Nus factors are also utilized by the phage HK022 Nun protein, an ARM protein related to N, to arrest transcription on the  $\lambda$  chromosome (11,16,17).

NusA is essential in wild-type *E. coli* (18,19) but not in *E. coli* deleted for cryptic prophage (20). In addition to promoting anti-termination, it enhances RNAP pausing (21,22) and termination (23,24). These reactions may be

\*To whom correspondence should be addressed. Tel: +49 921 55 3862; Fax: +49 921 553544; Email: stefan.prasch@uni-bayreuth.de

promoted by contacts between NusA and the 3'OH end of nascent RNA (25). NusA consists of five functional sub-domains: an N-terminal domain that interacts with RNAP (26), three RNA-binding domains, S1, KH1 and KH2 (8,27,28) and two C-terminal acidic domains, AR1 and AR2, that interact with  $\lambda$  N and the  $\alpha$  subunit of RNAP, respectively (Figure 1C) (17,29,30). AR2 masks one or more of the RNA-binding domains, thereby preventing NusA interaction with RNA (31). Structures of homologous NusA proteins from *Thermotoga maritima* (*T. maritima*) and from *M. tuberculosis* were determined in the absence and presence of RNA, respectively. Both structures show NusA to be highly elongated (8,27,28). Although knowledge of NusA has increased in recent years, several key questions are still open: Does *E. coli* NusA bind specifically or non-specifically to RNA? What *rrn* or *nut* sequences are critical for NusA binding? Are there structural differences between the NusA-*rrn* and NusA-*nut* RNA complexes?

## MATERIALS AND METHODS

### Buffers and reagents

All fluorescence titrations were performed in 50 mM potassium phosphate, 100 mM NaCl, 10 mM  $\beta$ -mercaptoethanol, pH 7.6, unless otherwise stated. Oligodeoxynucleotides as well as fluorescently-labeled oligoribonucleotides were obtained from biomers.net (Ulm, Germany; Table 1) and used according to the manufacturer's instructions.

### Plasmid construct, expression and protein purification

The DNA sequence of the NusA RNA-binding domains from amino acid 132 to 348 (NusA-SKK) was cloned via the BamHI and NdeI restriction sites into the *E. coli* expression vector pET11a (Novagen). The soluble recombinant NusA-SKK protein contained an N-terminal 5 $\times$ His tag. NusA-SKK was expressed and purified according to published procedures (31). Briefly, *E. coli* strain BL21 (DE3) (Novagen) harboring the recombinant plasmid was grown at 37°C in LB medium (Luria-Bertani) containing ampicillin (100  $\mu$ g/ml) until OD<sub>600</sub> = 0.5 and then induced with 0.1 mM isopropyl 1-thio- $\beta$ -D-galactopyranoside (IPTG). Cells were harvested 4 h after induction, lysed and purified as described (31). Finally, the protein was dialyzed against buffer as used for fluorescence measurements. The dialyzed protein was concentrated with Vivaspin concentrators (Vivascience, MWCO 10 000 Da). The identity and structural integrity of purified protein was analyzed by 19% SDS-PAGE as well as by CD- and NMR spectroscopy.

### NMR spectroscopy

NMR spectra were recorded on Bruker DRX 600 MHz spectrometers with triple-resonance probes equipped with pulsed field-gradient capabilities. The sample temperature was 298 K. 1D <sup>1</sup>H spectra were collected with water suppression using a 1-1 spin-echo pulse sequence including gradients.

## Fluorescence equilibrium measurements

We used various RNA sequences corresponding to  $\lambda$  *nut* to *rrnG boxA* sequence (*rrn BoxA*) of the *E. coli* genome (Table 1). Fluorescence equilibrium titrations were performed using an L-format Jobin-Yvon Horiba Fluoromax fluorimeter equipped with an automatic titration device (Hamilton). Extrinsic fluorescence measurements with 3' 6-carboxy-fluorescein (6-FAM)-labeled RNA were performed in fluorescence buffer as above in a total volume of 1 ml using a 10  $\times$  4 mm quartz cuvette (Hellma GmbH, Mühlheim, Germany). The excitation wavelength was 492 nm, and the emission intensity was measured at 516 nm applying a 500 nm cutoff filter. For anisotropic measurements, slit widths were set at 4.5 nm and 3.5 nm for excitation and emission, respectively. All titration measurements were performed at 25°C with 50 nM of fluorescently-labeled RNA. Following sample equilibration, at least six data points with an integration time of 0.8 s were collected for each titration point in the case of anisotropic measurements.

### Data fitting

Isotropic as well as anisotropic data were fitted to a two-state binding equation to determine the equilibrium dissociation constant ( $K_d$ ) using standard software. The anisotropy was calculated from:

$$A = f_{\text{complex}}A_{\text{complex}} + f_{\text{RNA}}A_{\text{RNA}} \quad 1$$

where  $A$ ,  $A_{\text{complex}}$  and  $A_{\text{RNA}}$  are the anisotropy values and  $f_{\text{complex}}$ ,  $f_{\text{RNA}}$  are the fractional intensities. The change in fluorescence intensity has to be taken into account, so that the bound fraction is given by

$$\frac{[\text{complex}]}{[\text{RNA}]_0} = \frac{A - A_{\text{RNA}}}{(A - A_{\text{RNA}}) + R(A_{\text{complex}} - A)} \quad 2$$

with

$$[\text{complex}] = \frac{(K_d + [P]_0 + [\text{RNA}]_0)}{2[\text{RNA}]_0} - \frac{\sqrt{(K_d + [P]_0 + [\text{RNA}]_0)^2 - 4[P]_0[\text{RNA}]_0}}{2[\text{RNA}]_0} \quad 3$$

where  $A$  is the anisotropy;  $A_{\text{RNA}}$  is the initial free anisotropy,  $A_{\text{complex}}$  is the anisotropy of the protein-RNA complex and  $P_0$  and  $\text{RNA}_0$  represent the total protein and RNA concentrations, respectively.  $R$  is the ratio of intensities of the bound and free forms.

## RESULTS

The *E. coli* NusA protein includes a C-terminal domain that masks the RNA-binding region (17,26,29,31). To determine the interaction of *E. coli* NusA with different RNA substrates, we used a NusA construct (NusA-SKK) lacking the two acidic-repeat C-terminal domains AR1 and AR2, as well as the N-terminal domain (Figure 1C). These regions are not directly involved in RNA binding. Thus, *E. coli* NusA416, deleted for AR2, forms complexes

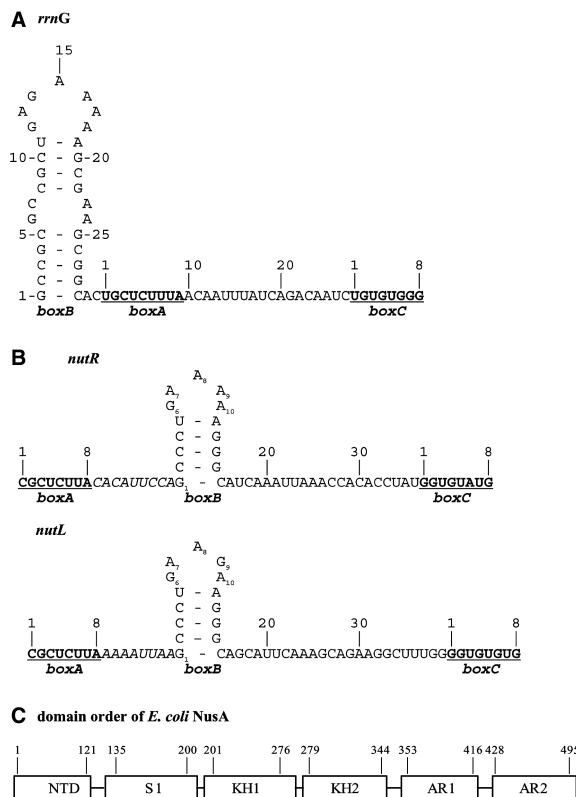


**Figure 1.** Different anti-terminator signal sequences. (A) *rrnG* leader sequence of *E. coli*. *boxB*, *boxA* and *boxC* refer to the  $\lambda$ -like anti-terminator (AT) features. Each box sequence is numbered separately; *boxA* and *boxC* are underlined. (B) Phage  $\lambda$  *nut* anti-termination sequence.  $\lambda$ *nutR* and  $\lambda$ *nutL* differ in the sequence and length of the *spacer* between *boxA* and *boxB*, as well as position 9 in the loop region of *boxB*. (C) Domain order of *E. coli* NusA. The numbers show the borders of the six domains: N-terminal domain (NTD), S1 domain (S1), K-homologous domain (KH), acidic repeat (AR).

with the *rrnG* leader region as well as with the *M. tuberculosis nut* RNA. Electrophoretic mobility-shift assays (EMSA) showed that the truncated *E. coli* NusA protein bound *nut*-like RNA species with high affinity, whereas the specificity was significantly lower than that of the *M. tuberculosis* NusA (7). This prompted us to investigate the affinity of different RNA species to *E. coli* NusA using fluorescence measurements. To avoid possible false negatives due to protein binding too distal to the fluorescence dye to alter fluorescence signal intensity, we used anisotropic fluorescence titrations instead of isotropic fluorescence measurements. Fluorescence anisotropy can detect molecular interactions even when an isotropic fluorescence signal change is weak or absent (32). Furthermore, changes of the fluorophore environment can be neglected with anisotropic measurements since the results are related to the rotational correlation time of a macromolecule with a rigidly attached fluorophore (33).

#### An extended *rrn boxA* sequence has the highest affinity to NusA-SKK

We first turned our attention to three different RNA species, the *rrnG* anti-terminator region,  $\lambda$ *nutL* and  $\lambda$  *nutR*, all of which interact with NusA and the other Nus factors (4).

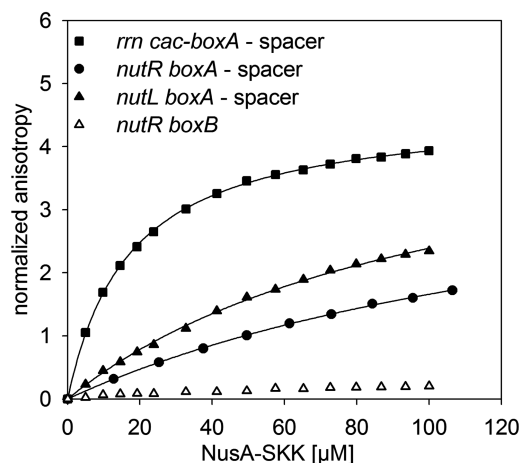


**Figure 2.** Fluorescence anisotropy measurements with homologous *nut*-RNAs. 50 nM *rrn boxA-spacer* (filled square),  $\lambda$ *nutR boxA-spacer* (filled circles),  $\lambda$ *nutL boxA-spacer* (filled triangles) and  $\lambda$ *nutR boxB* (open triangles) were titrated with NusA-SKK. The extrinsic fluorescence of the 3' 6-FAM label of the RNAs was determined. The curves show the best fit to Equation (3) (see 'Materials and Methods' section).  $K_d$  values of 14  $\mu$ M, 126  $\mu$ M, 71  $\mu$ M were determined, respectively (solid line; see Table 1). No  $K_d$  values could be fitted to  $\lambda$ *nutR boxB*.

*rrn* carries a stem-loop structure (*boxB*), *boxA* and *boxC* sequences. The *boxB* and *boxC* sequences of *rrn* are not required for anti-termination (1).

The *boxA* sequence of *rrn* differs from that of  $\lambda$  at the initial base and by the insertion of an additional U residue at the penultimate site, converting the *rrn boxA* to a consensus site. Conversion of  $\lambda$ *boxA* to consensus enhances N activity (34). The *spacer* sequence of *rrn* differs from both  $\lambda$ *nutL* and  $\lambda$ *nutR*, but all three *spacers* carry a conserved sequence of AUU (Figure 1). Interestingly, we find that the *rrn cac-boxA-spacer* sequence, which includes a CAC sequence just upstream to *boxA*, binds with higher affinity to NusA-SKK ( $K_d = 14 \mu$ M; Figure 2; Table 1) than either the  $\lambda$ *nutR boxA-spacer* (126  $\mu$ M) or the  $\lambda$ *nutL boxA-spacer* (71  $\mu$ M; Figure 2; Table 1).

#### Role of *boxA* flanking sequences in binding of NusA-SKK

In these experiments, we tested *boxA* sequences with flanking regions (Table 1). In the case of *rrn*, these included sequences between *boxB* and *boxA* (in capital letter), as well as sequences between *boxA* and *boxC* (*spacer*, in italics). In the case of phage  $\lambda$ *nutL* and  $\lambda$ *nutR*, the *spacer* separates *boxA* from *boxB*. We proceeded to further define the NusA-SKK interaction regions at  $\lambda$ *nutR*,  $\lambda$ *nutL* and *rrn*.

In the case of the  $\lambda$ *nut* sites, we find that the  $\lambda$ *nutL spacer* binds to NusA-SKK (24  $\mu$ M), whereas *boxA* alone shows no association with the protein (Figure 3A). Similarly, the *nutR spacer* binds NusA-SKK with an affinity nearly identical to that of *nutR boxA-spacer* ( $K_d$  value  $\sim 137 \mu$ M; Figure 3B), whereas NusA-SKK binding to *boxA* could not be detected.

To validate this result, we analyzed *nutR boxA-spacer* sequences with mutations in the *boxA* region (34,35). The *boxA5* and *boxA16* mutations decrease N activity,



**Table 1.** 3'-6-carboxyfluorescein (6-Fam)-labeled RNA oligonucleotides used in this study

Oligonucleotide	Sequence	$K_d$ for NusA-SKK ( $\mu\text{M}$ )
<i>nutR boxA-spacer</i>	5'- <b>cg</b> <u>cuuu</u> <b>acac</b> <i>auuuca</i> -3'	126 $\pm$ 4
<i>nutL boxA-spacer</i>	5'- <b>cg</b> <u>cuuu</u> <b>aaaa</b> <i>uuua</i> -3'	71 $\pm$ 4
<i>rrn cac-boxA-spacer</i>	5'-CAC <b>cg</b> <u>cuuu</u> <b>aa</b> <i>cauuua</i> -3'	14 $\pm$ 0.2
<i>nutR boxA</i>	5'- <b>cg</b> <u>cuuu</u> <b>a</b> -3'	n.d.
<i>nutR spacer</i>	5'- <b>ca</b> <u>cauu</u> <b>cca</b> -3'	137 $\pm$ 17
<i>nutL spacer</i>	5'- <b>aa</b> <u>uuuu</u> <b>a</b> -3'	24 $\pm$ 2.2
<i>nutR boxA5-spacer</i>	5'- <b>cu</b> <u>uuuu</u> <b>acac</b> <i>auuuca</i> -3'	124 $\pm$ 7
<i>nutR boxA16-spacer</i>	5'- <b>cg</b> <u>uuuu</u> <b>acac</b> <i>auuuca</i> -3'	106 $\pm$ 4
<i>nutR boxA69-spacer</i>	5'- <b>au</b> <u>agcg</u> <b>gc</b> <u>gcac</u> <i>uuca</i> -3'	n.d.
<i>nutL boxA-spacer (mut)</i>	5'- <b>cg</b> <u>cuuu</u> <b>aaaa</b> <u>agg</u> <i>aa</i> -3'	n.d.
<i>rrn boxA</i>	5'- <b>ug</b> <u>cuuu</u> <b>uu</b> <b>a</b> -3'	194 $\pm$ 38
<i>rrn-upstream-boxA' (I)</i>	5'-CAC <b>cg</b> <u>uc</u> <b>c</b> -3'	26 $\pm$ 0.8
<i>rrn-upstream (II)</i>	5'-AGCGGCAC-3'	30 $\pm$ 1.9
<i>rrn spacer (III)</i>	5'- <b>aca</b> <u>uuuu</u> <b>a</b> -3'	71 $\pm$ 3.3
<i>nutR boxB</i>	5'-agccuguaaaaaagggc-3'	n.d.

*boxA* nucleotides are shown in bold. Mutated nucleotides are underlined. Flanking regions of *rrn-boxA* are in capital letters. The *spacer* is shown in italic.

whereas the *boxA69* mutation has little effect on anti-termination (36). Fluorescence titrations of the three mutant RNAs indicate that only *boxA69* significantly increased the  $K_d$  value ( $>200 \mu\text{M}$ ) for NusA-SKK complex formation, whereas *boxA5* and *boxA16* exhibited  $K_d$  values similar to that of wild-type *boxA* ( $\sim 120 \mu\text{M}$ ; Figure 4A). These data demonstrate that *boxA* mutations that affect anti-termination have a very limited effect on NusA-SKK binding. Their phenotype instead may reflect a failure to bind NusB (37). Why  $\lambda\text{nutR } boxA69\text{-spacer}$  binds NusA-SKK less efficiently than  $\lambda\text{nutR } spacer$  alone is unclear, although a similar result was reported by Mah *et al.* (31) for a  $\lambda\text{nut}$  containing a reversed *boxA*. Furthermore, we also tested a mutation in the  $\lambda\text{nutL } spacer$  that replaces residues U13 and U14 that are conserved at both  $\lambda\text{nutR}$  and  $\lambda\text{nutL}$  (Figure 1B). This conservation suggests that these bases are important for binding of interaction partners. Indeed, transversion of these residues to G completely abolished NusA binding to *nutL-spacer* (Figure 4B).

We extended our analysis to the *rrn* anti-termination region, examining the binding affinities of RNA sequences upstream and downstream to *boxA* as well as *boxA* itself (Table 1). First, we found that *rrn boxA* showed no binding to NusA-SKK (Table 1). However, RNA that included an upstream CAC, as well as the first five bases of *boxA* was bound with high affinity ( $26 \pm 0.8 \mu\text{M}$ ), as was the 8 bases upstream of *boxA* (AGCGGCAC,  $30 \pm 1.9 \mu\text{M}$ ; Figure 3C). The *rrn spacer* also bound NusA-SKK with an affinity intermediate between that of  $\lambda\text{nutR } spacer$  and  $\lambda\text{nutL } spacer$  ( $71 \pm 3.3 \mu\text{M}$ ). Alignment with ClustalW2 of *rrn*,  $\lambda\text{nutL}$ , and  $\lambda\text{nutR}$  shows a conserved sequence, 5'-uuu-3', in all three *spacers*.

### $\lambda\text{boxB}$ does not interact with NusA-SKK

In contrast to *boxA* and flanking sequences, titration of  $\lambda\text{nutR } boxB$  with NusA-SKK, showed no, or only

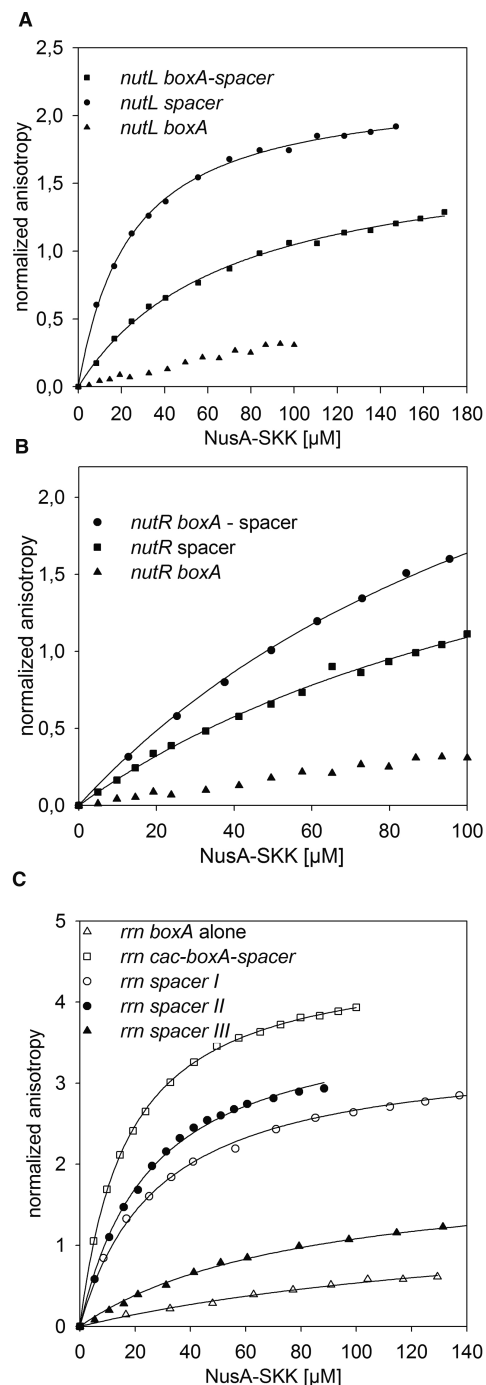


**Figure 3.** Fluorescence anisotropy measurements with separated RNAs regions. In each titration 50 nM of 6-FAM-labeled RNA was used. (A) 50 nM of 6-FAM-labeled  $\lambda\text{nutL } boxA\text{-spacer}$  (squares),  $\lambda\text{nutL } spacer$  (circles),  $\lambda\text{nutL } boxA$  (triangles) were titrated with NusA-SKK.  $K_d$  values of  $71 \mu\text{M}$  and  $24 \mu\text{M}$  were determined for  $\lambda\text{nutL } boxA\text{-spacer}$ ,  $\lambda\text{nutL } spacer$ , respectively (solid lines). No  $K_d$  value could be fitted to  $\lambda\text{nutL } boxA$  (see Table 1). (B) 50 nM of 6-FAM-labeled  $\lambda\text{nutR } boxA\text{-spacer}$  (circles),  $\lambda\text{nutR } spacer$  (squares),  $\lambda\text{nutR } boxA$  (triangles) were titrated with NusA-SKK.  $K_d$  values of  $126 \mu\text{M}$  and  $137 \mu\text{M}$  were determined for  $\lambda\text{nutR } boxA\text{-spacer}$ ,  $\lambda\text{nutR } spacer$ , respectively (solid lines). No  $K_d$  value could be fitted to  $\lambda\text{nutR } boxA$  (see Table 1). (C) 50 nM of 6-FAM-labeled *rrn boxA* alone (open triangle), *rrn cac-boxA-spacer* (open square), *rrn spacer I* (open circle), *rrn spacer II* (filled circle), *rrn spacer III* (filled triangle) were titrated with NusA-SKK.  $K_d$  values can be seen in Table 1. No  $K_d$  value could be fitted to *rrn boxA* (see Table 1).

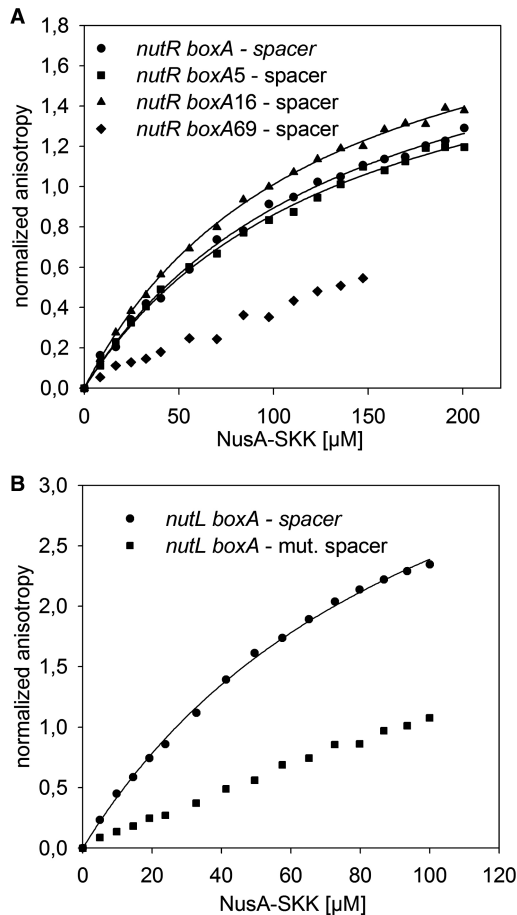


**Figure 4.** Fluorescence anisotropy measurements with mutated  $\lambda\text{nut}$  *boxA* RNA. (A) 50 nM of 6-FAM-labeled  $\lambda\text{nutR}$  *boxA*-*spacer* (circles),  $\lambda\text{nutR}$  *boxA5*-*spacer* (squares),  $\lambda\text{nutR}$  *boxA16*-*spacer* (triangles), or  $\lambda\text{nutR}$  *boxA69*-*spacer* (diamonds) were titrated with NusA-SKK.  $K_d$  values of 126  $\mu\text{M}$ , 124  $\mu\text{M}$ , 106  $\mu\text{M}$  were determined, respectively (solid lines; see Table 1). No  $K_d$  values could be fitted to  $\lambda\text{nutR}$  *boxA69* (see Table 1). (B) 50 nM of 6-FAM-labeled  $\lambda\text{nutL}$  *boxA*-*spacer* (circles),  $\lambda\text{nutL}$  *mut. spacer* (squares) were titrated with NusA-SKK.  $K_d$  value of 71  $\mu\text{M}$  was determined for *nutL boxA-spacer* (solid lines). No  $K_d$  value could be fitted to *nutL boxA-mut-spacer* (see Table 1).

very weak, nonspecific protein–RNA interactions (Figure 5). To confirm that  $\lambda\text{nutR}$  *boxB* does not interact with NusA-SKK, even at higher concentrations, we analyzed a sample containing both species with 1D-NMR. In contrast to  $\lambda\text{nutR}$  *boxA*,  $\lambda\text{nutR}$  *boxB* forms a stable stem-loop structure allowing the detection of the slowly exchanging imino protons in the double-stranded stem region. The 1D-NMR spectrum of NusA-SKK in the absence of RNA shows a well-dispersed amide proton signal region, indicating a stably folded, highly structured protein (Figure 5A). The  $\lambda\text{nutR}$  *boxB* 1D-NMR spectrum reveals signals in the range of 12–14 p.p.m., corresponding to the imino protons of the stem region (Figure 5B). Interaction between the stem region of  $\lambda\text{nutR}$  *boxB* and NusA-SKK, would affect these readily observable imino proton signals. The observable signals, however, of both protein and RNA, were unchanged when incubated together, clearly indicating that no complex forms between NusA-SKK

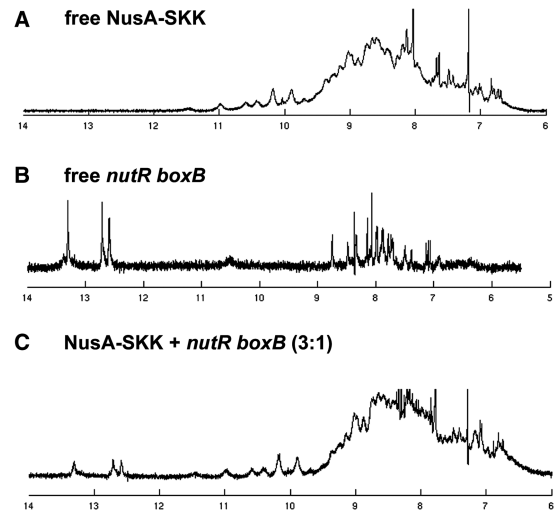


**Figure 5.** 1D-NMR analysis. Imino proton region of NusA-SKK (175  $\mu\text{M}$ ; A),  $\lambda\text{nutR}$  *boxB* (100  $\mu\text{M}$ ; B) and NusA-SKK +  $\lambda\text{nutR}$  *boxB* (3:1; C).

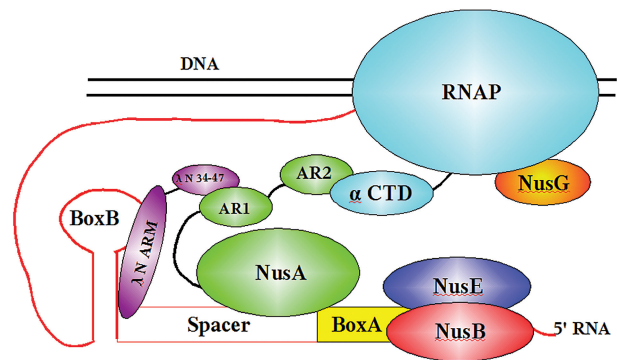


**Figure 6.** Model of the anti-termination network. The interaction of the RNAP with various factors important for anti-termination (see text for details).

and  $\lambda\text{nutR}$  *boxB* even at NusA concentrations in the high micromolar range (Figure 5C). The observed signal increase is due to the lower concentration of  $\lambda\text{nutR}$  RNA after addition of NusA-SKK.

## CONCLUSIONS

Mutational studies indicated that NusA as well as *boxA* play an important role in anti-termination (38,39). *boxA* forms a complex with NusB/NusE (5,6,37) and it was suggested that NusA links  $\lambda\text{nut}$  *boxA* and  $\lambda\text{nut}$  *boxB* by binding to both (37,40). Oddly, however, and in contrast to *boxA* point mutations, anti-termination was still efficient, and NusB-independent, in a *boxA* deletion mutant (36,41). Additionally, deletion of the initial three bases (*cac*) of the  $\lambda\text{nutR}$  *spacer* did not affect anti-termination, whereas deletion of the initial six bases (*cacauu*) led to complete loss of anti-termination activity. In agreement with the X-ray structure of *M. tuberculosis* NusA with RNA and deletion studies, our fluorescence analyses

revealed that NusA recognizes a *spacer* sequence that includes the critical bases AUU (8,36). NusA interaction with the *rrn*,  $\lambda$ *nutL* and  $\lambda$ *nutR* *boxA-spacer* motif was demonstrated by mutational studies and *in vitro* binding assays (1,37,39,42), and NusA was also suggested to recognize RNA outside the  $\lambda$ *nut* region (19,27,37,43). Complex formation between NusA and *spacer* might promote binding of NusE/NusB to the adjacent *boxA* sequence, and the notion that NusA binds to the  $\lambda$ *nut* *spacer* region is now strongly supported by the present fluorescence titration data.

Differences between the *rrn* anti-terminator regions and  $\lambda$ *nut* have already been described (5,37). Berg *et al.* (1) showed that *rrn boxA-spacer* plus seven upstream residues were sufficient to suppress termination at Rho-dependent terminators. We show here that the upstream CAC sequence as well as the downstream *spacer*, bind NusA-SKK. This redundancy may be related to the fact that  $\lambda$ *nut*-dependent anti-termination, which suppresses both Rho-dependent and Rho-independent terminators, requires  $\lambda$ N and *boxB*, whereas *rrn* anti-termination requires neither (37,44). In addition to greater anti-termination efficiency, the requirement for  $\lambda$ N and *BoxB* allows regulation of  $\lambda$  anti-termination. Thus,  $\lambda$  N levels are controlled at the levels of transcription, translation and protein stability (45,46).

Note that the NusE/NusB complex binds to *boxA* with affinities in the nanomolar range (5), whereas the  $K_d$  values for NusA-SKK are in the micromolar range. We suggest that tight RNA binding by NusA may not be required since it is already bound to RNAP and thus in close vicinity to nascent RNA. The  $\lambda$ *nutL* *spacer* sequence differs from that of  $\lambda$ *nutR* *spacer* (Table 1), and this difference is thought to account in part for the enhanced efficiency of Nus-mediated termination at  $\lambda$ *nutL* relative to  $\lambda$ *nutR* (Washburn, R.S. and Gottesman, M.E., unpublished data), and  $\lambda$ *nutL* *boxA-spacer* binds with significantly higher affinity to NusA-SKK than does  $\lambda$ *nutR* *boxA-spacer*. Both *spacer* sequences contain U's at residues 13 and 14, implying that these bases are important interaction partners. As shown above, replacement of the U's with G's completely abolished NusA-SKK binding to  $\lambda$ *nutL-spacer*. From this and other data, the following picture of the assembly of the anti-termination complex at the  $\lambda$ *nut* RNA has evolved (Figure 6): After RNAP has synthesized  $\lambda$ *nut* RNA, NusE and NusB bind to *boxA*, and NusA binds to *spacer* facilitated by NusA AR2 interaction with the C-terminal domain of the  $\alpha$  subunit of RNAP.  $\lambda$ N protein binds to AR1 of NusA as demonstrated for N(34-47) (17,30), forming a weak helix at the protein's N-terminus (17). This weak helix facilitates recognition of *boxB* (17). NusA interaction with RNA is thus stabilized by the AR2:RNAP interaction as well as by the AR1:N:*boxB* interaction, relieving the requirement for tight binding of NusA to  $\lambda$ *nut*.

## ACKNOWLEDGEMENTS

P.R. would like to thank the Columbia University Microbiology Department for their patience during his sabbatical stay in New York.

## FUNDING

The Deutsche Forschungsgemeinschaft DFG (Ro617/16-1 to B.M.W. and P.R.); and the NIH (NIGMS R01/GM37219 to M.E.G.).

*Conflict of interest statement.* None declared.

## REFERENCES

- Berg, K.L., Squires, C. and Squires, C.L. (1989) Ribosomal RNA operon anti-termination. function of leader and spacer region box B-box A sequences and their conservation in diverse micro-organisms. *J. Mol. Biol.*, **209**, 345–358.
- Friedman, D.I. and Court, D.L. (1995) Transcription anti-termination: the lambda paradigm updated. *Mol. Microbiol.*, **18**, 191–200.
- Weisberg, R.A. and Gottesman, M.E. (1999) Processive anti-termination. *J. Bacteriol.*, **181**, 359–367.
- Squires, C.L., Greenblatt, J., Li, J., Condon, C. and Squires, C.L. (1993) Ribosomal RNA antitermination *in vitro*: requirement for nus factors and one or more unidentified cellular components. *Proc. Natl Acad. Sci. USA*, **90**, 970–974.
- Greive, S.J., Lins, A.F. and von Hippel, P.H. (2005) Assembly of an RNA-protein complex. binding of NusB and NusE (S10) proteins to *boxA* RNA nucleates the formation of the antitermination complex involved in controlling rRNA transcription in *Escherichia coli*. *J. Biol. Chem.*, **280**, 36397–36408.
- Luo, X., Hsiao, H.H., Bubunenko, M., Weber, G., Court, D.L., Gottesman, M.E., Urlaub, H. and Wahl, M.C. (2008) Structural and functional analysis of the *E. coli* NusB-S10 transcription antitermination complex. *Mol. Cell*, **32**, 791–802.
- Arnvig, K.B., Pennell, S., Gopal, B. and Colston, M.J. (2004) A high-affinity interaction between NusA and the *rrn* nut site in *Mycobacterium tuberculosis*. *Proc. Natl Acad. Sci. USA*, **101**, 8325–8330.
- Beuth, B., Pennell, S., Arnvig, K.B., Martin, S.R. and Taylor, I.A. (2005) Structure of a *Mycobacterium tuberculosis* NusA-RNA complex. *EMBO J.*, **24**, 3576–3587.
- Friedman, D.I., Olson, E.R., Johnson, L.L., Alessi, D. and Craven, M.G. (1990) Transcription-dependent competition for a host factor: the function and optimal sequence of the phage lambda *boxA* transcription antitermination signal. *Genes Dev.*, **4**, 2210–2222.
- Friedman, D.I. and Baron, L.S. (1974) Genetic characterization of a bacterial locus involved in the activity of the N function of phage lambda. *Virology*, **58**, 141–148.
- Nudler, E. and Gottesman, M.E. (2002) Transcription termination and anti-termination in *E. coli*. *Genes Cells*, **7**, 755–768.
- Schärfp, M., Sticht, H., Schweimer, K., Boehm, M., Hoffmann, S. and Rösch, P. (2000) Antitermination in bacteriophage lambda. the structure of the N36 peptide-*boxB* RNA complex. *Eur. J. Biochem.*, **267**, 2397–408.
- Legault, P., Li, J., Mogridge, J., Kay, L.E. and Greenblatt, J. (1998) NMR structure of the bacteriophage lambda N peptide/*boxB* RNA complex: recognition of a GNRA fold by an arginine-rich motif. *Cell*, **93**, 289–299.
- Das, A. and Wolska, K. (1984) Transcription antitermination *in vitro* by lambda N gene product: requirement for a phage nut site and the products of host nusA, nusB, and nusE genes. *Cell*, **38**, 165–173.
- Condon, C., Squires, C. and Squires, C.L. (1995) Control of rRNA transcription in *Escherichia coli*. *Microbiol. Rev.*, **59**, 623–645.
- Robert, J., Sloan, S.B., Weisberg, R.A., Gottesman, M.E., Robledo, R. and Harbrecht, D. (1987) The remarkable specificity of a new transcription termination factor suggests that the mechanisms of termination and antitermination are similar. *Cell*, **51**, 483–492.
- Prasch, S., Schwarz, S., Eisenmann, A., Wöhr, B.M., Schweimer, K. and Rösch, P. (2006) Interaction of the intrinsically unstructured phage lambda N protein with *Escherichia coli* NusA. *Biochemistry*, **45**, 4542–4549.
- Zhou, Y., Mah, T.F., Yu, Y.T., Mogridge, J., Olson, E.R., Greenblatt, J. and Friedman, D.I. (2001) Interactions of an arg-rich region of transcription elongation protein NusA with NUT



- RNA: implications for the order of assembly of the lambda N antitermination complex in vivo. *J. Mol. Biol.*, **310**, 33–49.
19. Zhou, Y., Mah, T.F., Greenblatt, J. and Friedman, D.I. (2002) Evidence that the KH RNA-binding domains influence the action of the *E. coli* NusA protein. *J. Mol. Biol.*, **318**, 1175–1188.
  20. Cardinale, C.J., Washburn, R.S., Tadigotla, V.R., Brown, L.M., Gottesman, M.E. and Nudler, E. (2008) Termination factor rho and its cofactors NusA and NusG silence foreign DNA in *E. coli*. *Science*, **320**, 935–938.
  21. Landick, R. and Yanofsky, C. (1987) Isolation and structural analysis of the *Escherichia coli* trp leader paused transcription complex. *J. Mol. Biol.*, **196**, 363–377.
  22. Chan, C.L. and Landick, R. (1993) Dissection of the his leader pause site by base substitution reveals a multipartite signal that includes a pause RNA hairpin. *J. Mol. Biol.*, **233**, 25–42.
  23. Farnham, P.J., Greenblatt, J. and Platt, T. (1982) Effects of NusA protein on transcription termination in the tryptophan operon of *Escherichia coli*. *Cell*, **29**, 945–951.
  24. Schmidt, M.C. and Chamberlin, M.J. (1987) nusA protein of *Escherichia coli* is an efficient transcription termination factor for certain terminator sites. *J. Mol. Biol.*, **195**, 809–818.
  25. Liu, K. and Hanna, M.M. (1995) NusA contacts nascent RNA in *Escherichia coli* transcription complexes. *J. Mol. Biol.*, **247**, 547–558.
  26. Mah, T.F., Li, J., Davidson, A.R. and Greenblatt, J. (1999) Functional importance of regions in *Escherichia coli* elongation factor NusA that interact with RNA polymerase, the bacteriophage lambda N protein and RNA. *Mol. Microbiol.*, **34**, 523–537.
  27. Worbs, M., Bourenkov, G.P., Bartunik, H.D., Huber, R. and Wahl, M.C. (2001) An extended RNA binding surface through arrayed S1 and KH domains in transcription factor NusA. *Mol. Cell*, **7**, 1177–1189.
  28. Gopal, B., Haire, L.F., Gamblin, S.J., Dodson, E.J., Lane, A.N., Papavasiasundaram, K.G., Colston, M.J. and Dodson, G. (2001) Crystal structure of the transcription elongation/anti-termination factor NusA from *Mycobacterium tuberculosis* at 1.7 Å resolution. *J. Mol. Biol.*, **314**, 1087–1095.
  29. Eisenmann, A., Schwarz, S., Prasch, S., Schweimer, K. and Rösch, P. (2005) The *E. coli* NusA carboxy-terminal domains are structurally similar and show specific RNAP- and  $\lambda$  N interaction. *Protein Sci.*, **14**, 2018–2029.
  30. Bonin, I., Muhlberger, R., Bourenkov, G.P., Huber, R., Bacher, A., Richter, G. and Wahl, M.C. (2004) Structural basis for the interaction of *Escherichia coli* NusA with protein N of phage lambda. *Proc. Natl Acad. Sci. USA*, **101**, 13762–13767.
  31. Mah, T.F., Kuznedelov, K., Mushegian, A., Severinov, K. and Greenblatt, J. (2000) The alpha subunit of *E. coli* RNA polymerase activates RNA binding by NusA. *Genes Dev.*, **14**, 2664–2675.
  32. Takahashi, M., Sakumi, K. and Sekiguchi, M. (1990) Interaction of ada protein with DNA examined by fluorescence anisotropy of the protein. *Biochemistry*, **29**, 3431–3436.
  33. Cantor, C.R. and Schimmel, P.R. (1981) *Biophysical Chemistry*. Freeman, San Francisco, pp. 454–465.
  34. Olson, E.R., Tomich, C.S. and Friedman, D.I. (1984) The nusA recognition site: alteration in its sequence or position relative to upstream translation interferes with the action of the N antitermination function of phage lambda. *J. Mol. Biol.*, **180**, 1053–1063.
  35. Robledo, R., Gottesman, M.E. and Weisberg, R.A. (1990) Lambda nutR mutations convert HK022 nus protein from a transcription termination factor to a suppressor of termination. *J. Mol. Biol.*, **212**, 635–643.
  36. Zuber, M., Patterson, T.A. and Court, D.L. (1987) Analysis of nutR, a site required for transcription antitermination in phage lambda. *Proc. Natl Acad. Sci. USA*, **84**, 4514–4518.
  37. Mogridge, J., Mah, T.F. and Greenblatt, J. (1995) A protein-RNA interaction network facilitates the template-independent cooperative assembly on RNA polymerase of a stable antitermination complex containing the lambda N protein. *Genes Dev.*, **9**, 2831–2845.
  38. Olson, E.R., Flamm, E.L. and Friedman, D.I. (1982) Analysis of nutR: a region of phage lambda required for antitermination of transcription. *Cell*, **31**, 61–70.
  39. Friedman, D.I. and Olson, E.R. (1983) Evidence that a nucleotide sequence, 'boxA,' is involved in the action of the NusA protein. *Cell*, **34**, 143–149.
  40. Mogridge, J., Legault, P., Li, J., Van Oene, M.D., Kay, L.E. and Greenblatt, J. (1998) Independent ligand-induced folding of the RNA-binding domain and two functionally distinct antitermination regions in the phage lambda N protein. *Mol. Cell*, **1**, 265–275.
  41. Patterson, T.A., Zhang, Z., Baker, T., Johnson, L.L., Friedman, D.I. and Court, D.L. (1994) Bacteriophage lambda N-dependent transcription antitermination: competition for an RNA site may regulate antitermination. *J. Mol. Biol.*, **236**, 217–228.
  42. Schauer, A.T., Carver, D.L., Bigelow, B., Baron, L.S. and Friedman, D.I. (1987) Lambda N antitermination system: functional analysis of phage interactions with the host NusA protein. *J. Mol. Biol.*, **194**, 679–690.
  43. Tsugawa, A., Kurihara, T., Zuber, M., Court, D.L. and Nakamura, Y. (1985) *E. coli* NusA protein binds in vitro to an RNA sequence immediately upstream of the boxA signal of bacteriophage lambda. *EMBO J.*, **4**, 2337–2342.
  44. Morgan, E.A. (1986) Antitermination mechanisms in rRNA operons of *Escherichia coli*. *J. Bacteriol.*, **168**, 1–5.
  45. Wilson, H.R., Zhou, J.G., Yu, D. and Court, D.L. (2004) Translation repression by an RNA polymerase elongation complex. *Mol. Microbiol.*, **53**, 821–828.
  46. Gottesman, S., Gottesman, M., Shaw, J.E. and Pearson, M.L. (1981) Protein degradation in *E. coli*: the lon mutation and bacteriophage lambda N and cII protein stability. *Cell*, **24**, 225–233.